
The Spin–Orbit Resonances of the Solar System: A Mathematical Treatment Matching Physical Data

Francesco Antognini · Luca Biasco ·
Luigi Chierchia

Received: 9 July 2013 / Accepted: 21 January 2014
© Springer Science+Business Media New York 2014

Abstract In the mathematical framework of a restricted, slightly dissipative spin–orbit model, we prove the existence of periodic orbits for astronomical parameter values corresponding to *all* satellites of the Solar System observed in exact spin–orbit resonance.

Keywords Periodic orbits · Celestial mechanics · Spin–orbit resonances · Moons in the Solar System · Mercury · Dissipative systems

Mathematics Subject Classification 70F15 · 70F40 · 70E20 · 70G70 · 70H09 · 70H12 · 34C23 · 34C25 · 34C60 · 34D10

1 Introduction and Results

1.1 Satellites in Spin–Orbit Resonance

One of the many fascinating features of the Solar System is the presence of moons moving in a “synchronous” way around their planet, as experienced, for example,

Communicated by Amadeu Delshams.

F. Antognini
Departement Mathematik, ETH–Zürich, 8092 Zurich, Switzerland
e-mail: antognif@math.ethz.ch

L. Biasco · L. Chierchia (✉)
Dipartimento di Matematica e Fisica, Università “Roma Tre”, Largo S.L. Murialdo 1,
00146 Rome, Italy
e-mail: luigi@mat.uniroma3.it

L. Biasco
e-mail: biasco@mat.uniroma3.it

by earthlings looking always on the same, familiar face of their satellite. Indeed, 18 moons of our Solar System move in so-called 1:1 spin–orbit resonance: while performing a complete revolution on an (approximately) Keplerian ellipse around their principal body, they also complete a rotation around their spin axis (which is—again, approximately—perpendicular to the revolution plane); in this way, these moons always show the same side to their host planet.

The list of these 18 moons is as follows: Moon (Earth); Io, Europa, Ganymede, Callisto (Jupiter); Mimas, Enceladus, Tethys, Dione, Rhea, Titan, Iapetus (Saturn); Ariel, Umbriel, Titania, Oberon, Miranda (Uranus); Charon (Pluto); minor bodies with mean radius smaller than 100 km are not considered (see, however, Appendix 3).

There is only one more occurrence of spin–orbit resonance in the Solar System: the strange case of the 3:2 resonance of Mercury around the Sun (i.e., Mercury rotates three times on its spin axis, while making two orbital revolutions around the Sun).

In this paper we discuss a mathematical theory which is consistent with the existence of all spin–orbit resonances of the Solar System; in other words, we *prove a theorem*, in a framework of a well-known simple “restricted spin–orbit model,” establishing the existence of periodic orbits *for parameter values corresponding to all the satellites (or Mercury) in our Solar System* observed in spin–orbit resonance.

We remark that, in dealing with mathematical models trying to describe physical phenomena, one may be able to rigorously prove theorems only for parameter values, typically, somewhat smaller than the physical ones; on the other hand, for the true physical values, typically, one only obtains numerical evidence. In the present case, thanks to sharp estimates, we are able to fill such a gap and prove rigorous results for the real parameter values. Moreover, such results might also be an indication that the mathematical model adopted is quite effective in describing the physics.

1.2 The Mathematical Model

We consider a simple—albeit nontrivial—model in which the center of mass of the satellite moves on a given two-body Keplerian orbit focused on a massive point (primary body) exerting gravitational attraction on the body of the satellite modeled by a triaxial ellipsoid with equatorial axes $a \geq b > 0$ and polar axis c ; the spin polar axis is assumed to be perpendicular to the Keplerian orbit plane;¹ finally, we include also small dissipative effects (due to the possible internal nonrigid structure of the satellite), according to the “viscous-tidal model, with a linear dependence on the tidal frequency” (Correia and Laskar 2004): essentially, the dissipative term is given by the average over one revolution period of the so-called MacDonald’s torque (MacDonald 1964); compare (Peale 2005).

For a discussion of this model, see (Celletti 1990); for further references, see (Danby 1962; Goldreich and Peale 1967; Wisdom 1987; Celletti 2010); for a different [partial differential equation (PDE)] model, see (Bambusi and Haus 2012).

¹ The largest relative inclination (of the spin axis to the orbital plane) is that of Iapetus (8.298°) followed by Mercury (7°), Moon (5.145°), and Miranda (4.338°); all the other moons have inclination on the order of 1° or less.

The differential equation governing the motion of the satellite is then given by

$$\ddot{x} + \eta(\dot{x} - v) + \varepsilon f_x(x, t) = 0, \tag{1}$$

where:

- (a) x is the angle (mod 2π) formed by the direction of (say) the major equatorial axis of the satellite with the direction of the semi-major axis of the Keplerian ellipse plane; “dot” represents derivative with respect to t , where t (also defined mod 2π) is the mean anomaly (i.e., the ellipse area between the semi-major axis and the orbital radius ρ_e divided by the total area times 2π) and e is the eccentricity of the ellipse;
- (b) The dissipation parameters $\eta = K\Omega_e$ and $v = v_e$ are real-analytic functions of the eccentricity e : $K \geq 0$ is a physical constant depending on the internal (nonrigid) structure of the satellite, and²

$$\begin{aligned} \Omega_e &:= \left(1 + 3e^2 + \frac{3}{8}e^4\right) \frac{1}{(1 - e^2)^{9/2}}, \\ N_e &:= \left(1 + \frac{15}{2}e^2 + \frac{45}{8}e^4 + \frac{5}{16}e^6\right) \frac{1}{(1 - e^2)^6}, \\ v_e &:= \frac{N_e}{\Omega_e}. \end{aligned} \tag{2}$$

- (c) The constant ε measures the *oblateness* (or “equatorial ellipticity”) of the satellite and is defined as $\varepsilon = \frac{3}{2} \frac{B-A}{C}$, where $A \leq B$ and C are the principal moments of inertia of the satellite (C being referred to the polar axis);
- (d) The function f is the (“dimensionless”) Newtonian potential given by

$$f(x, t) := -\frac{1}{2\rho_e(t)^3} \cos(2x - 2f_e(t)), \tag{3}$$

where $\rho_e(t)$ and $f_e(t)$ are, respectively, the (normalized) orbital radius

$$\rho_e(t) := 1 - e \cos(u_e(t)) \tag{4}$$

and the polar angle (see³ Fig. 1); the eccentric anomaly $u = u_e(t)$ is defined implicitly by the Kepler equation⁴

$$t = u - e \sin(u). \tag{5}$$

² In [Correia and Laskar \(2004\)](#) (see Eq. 2) Ω_e and N_e are denoted, respectively, by $\Omega(e)$ and $N(e)$, while, in [Peale \(2005\)](#), they are denoted, respectively, by $f_1(e)$ and $f_2(e)$.

³ The analytic expression of the true anomaly in terms of the eccentric anomaly is given by $f_e(t) = 2 \arctan\left(\sqrt{\frac{1+e}{1-e}} \tan\left(\frac{u_e(t)}{2}\right)\right)$.

⁴ As is well known (see [Wintner 1941](#)), $e \rightarrow u_e(t)$ is, for every $t \in \mathbb{R}$, holomorphic for $|e| < r_*$, with $r_* := \max_{y \in \mathbb{R}} \frac{y}{\cosh(y)} = \frac{y_*}{\cosh(y_*)} = 0.6627434\dots$ and $y_* = 1.1996786\dots$

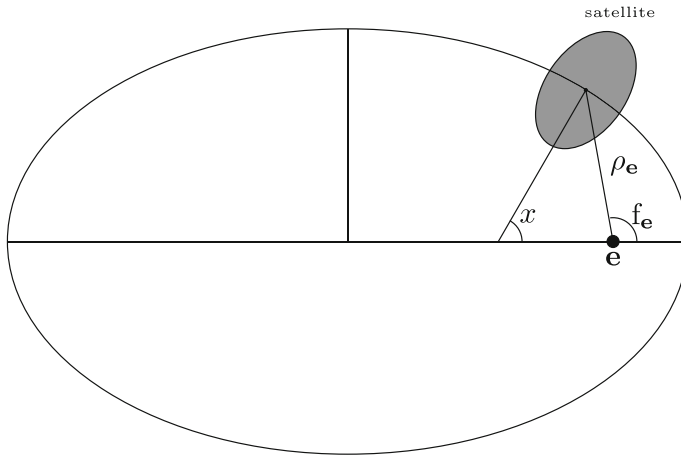


Fig. 1 Triaxial satellite revolving on a rescaled Keplerian ellipse (equatorial section)

Notice that the Newtonian potential $f(x, t)$ is a doubly periodic function of x and t , with periods 2π .

Remarks (i) The principal moments of an ellipsoid of mass m and with axes a , b , and c are given by

$$A = \frac{1}{5}m (b^2 + c^2), \quad B = \frac{1}{5}m (a^2 + c^2), \quad C = \frac{1}{5}m (a^2 + b^2).$$

The oblateness ε is then given by

$$\varepsilon = \frac{3B - A}{2C} = \frac{3a^2 - b^2}{2a^2 + b^2}. \tag{6}$$

(ii) There is no universally accepted determination of the internal rigidity constant K for most satellites of the Solar System.⁵ For the Moon and Mercury an accepted value is $\sim 10^{-8}$; see, e.g., (Celletti 1990). However, for our analysis to hold it will be enough that $\eta \leq 0.008$ for the moons and $\eta \leq 0.001$ for Mercury.

The known physical parameter values of the 18 moons of the Solar System needed for our analysis are reported in Table 1.⁶

The corresponding data for Mercury are presented in Table 2.

⁵ See, however, Iess et al. (2012), Hussmann et al. (2012), Lainey et al. (2012), and Castillo-Rogez et al. (2011).

⁶ $a \geq b$ denote the maximal and minimal observed equatorial radii, which, in our model, are assumed to be the axes of the ellipse modeling the equatorial section of the satellite. The dimensions of the polar radius are not relevant in our model; however, for all the cases considered in this paper it turns out to be always smaller than or equal to the smallest equatorial radius.

Table 1 Physical data of the moons in 1:1 spin-orbit resonance (http://ssd.jpl.nasa.gov/?sat_phys_par and http://ssd.jpl.nasa.gov/?sat_elem)

Principal body	Satellite	Eccentricity e	a (km)	b (km)	Oblateness $\varepsilon = \frac{3}{2} \frac{a^2 - b^2}{a^2 + b^2}$	ν
Earth	Moon ^a	0.0549	1740.19	1737.31	0.00248454179	1.018088056
Jupiter	Io ^b	0.0041	1829.7	1819.2	0.00863266715	1.00010086
	Europa	0.0094	1561.3	1560.3	0.00096104552	1.000530163
	Ganymede	0.0011	2632.9	2629.5	0.0019382783	1.00000726
	Callisto	0.0074	2411.8	2408.8	0.00186698679	1.000328561
Saturn	Mimas ^c	0.0193	208.3	196.2	0.08966019091	1.002234993
	Enceladus ^c	0.0047	257.2	251.2	0.03540026218	1.00013254
	Tethys ^c	0.0001	538.7	527.0	0.03293212897	1.00000006
	Dione ^c	0.0022	564.0	560.8	0.00853478156	1.00002904
	Rhea ^c	0.001	766.8	761.8	0.0098127957	1.000006
	Titan ^d	0.0288	2575.239	2574.932	0.00017882901	1.00497691
	Iapetus ^c	0.0283	748.9	743.1	0.011662022156	1.004805592
Uranus	Ariel ^e	0.0012	582.0	577.3	0.012162311957	1.00000864
	Umbriel ^e	0.0039	587.5	581.9	0.01436601227	1.00009126
	Titania ^e	0.0011	790.7	787.1	0.00684493838	1.00000726
	Oberon ^c	0.0014	764.0	758.8	0.01024416739	1.00001176
	Miranda ^c	0.0013	241.0	233.3	0.04869051956	1.00001014
Pluto	Charon ^f	0.0022	605.0	602.2	0.00695821306	1.00002904

^a Runcorn and Hofmann (1972)
^b Thomas et al. (1998)
^c Dougherty et al. (2009)
^d Iess et al. (2010)
^e Thomas (1988)
^f Sicardy et al. (2006)

Table 2 Physical data for Mercury in 3:2 spin-orbit resonance (<http://nssdc.gsfc.nasa.gov/planetary/factsheet/mercuryfact.html> and <http://solarsystem.nasa.gov/planets/chartchart.cfm>)

Principal body	Satellite	Eccentricity e	a (km)	b (km)	Oblateness $\varepsilon = \frac{3}{2} \frac{a^2 - b^2}{a^2 + b^2}$	ν
Sun	Mercury	0.2056	2440.7	2439.7	0.00061470369	1.255835458

1.3 Existence Theorem for Solar System Spin-Orbit Resonances

In this framework, a $p:q$ spin-orbit resonance (with p and q co-prime nonvanishing integers) is, by definition, a solution $t \in \mathbb{R} \rightarrow x(t) \in \mathbb{R}$ of (1) such that

$$x(t + 2\pi q) = x(t) + 2\pi p; \tag{7}$$

indeed, for such orbits, after q revolutions of the orbital radius, x has made p complete rotations.⁷

Our main result can, now, be stated as follows:

Theorem (Moons) *The differential equation (1) (a)–(d) admits spin–orbit resonances (7) with $p = q = 1$ provided \mathbf{e} , ν , and ε are as in Table 1 and $0 \leq \eta \leq 0.008$.*

(Mercury) *The differential equation (1) (a)–(d) admits spin–orbit resonances (7) with $p = 3$ and $q = 2$ provided \mathbf{e} , ν , and ε are as in Table 2 and $0 \leq \eta \leq 0.001$.*

In Biasco and Chierchia (2009) (compare Theorem 1.2), existence of spin–orbit resonances with $q = 1, 2, 4$ and any p (co-prime with q) is proved,⁸ while in Celletti and Chierchia (2009), quasi-periodic solutions corresponding to p/q irrational are studied in the same model. In Biasco and Chierchia (2009), no explicit computations of constants (size of admissible ε , size of admissible η , etc.) were carried out.

The main point of this paper is to compute all constants explicitly in order to get nearly optimal estimates and include *all* cases of physical interest.

2 Proof of the Theorem

2.1 Step 1: Reformulation of the Problem of Finding Spin–Orbit Resonances

Let $x(t)$ be a $p:q$ spin–orbit resonance and let $u(t) := x(qt) - pt - \xi$. Then, by (7) and choosing ξ suitably, one sees immediately that u is 2π -periodic and satisfies the differential equation

$$u''(t) + \hat{\eta} (u'(t) - \hat{\nu}) + \hat{\varepsilon} f_x(\xi + pt + u(t), qt) = 0, \quad \langle u \rangle = 0, \tag{8}$$

where $\langle \cdot \rangle$ denotes the average over the period⁹ and

$$\hat{\eta} := q\eta, \quad \hat{\nu} := q\nu - p, \quad \hat{\varepsilon} := q^2\varepsilon. \tag{9}$$

Separating the linear part from the nonlinear one, we can rewrite (8) as follows: let

$$\begin{cases} Lu := u'' + \hat{\eta} u' \\ [\Phi_\xi(u)](t) := \hat{\eta} \hat{\nu} - \hat{\varepsilon} f_x(\xi + pt + u(t), qt) \end{cases} \tag{10}$$

then, the differential equation in (8) is equivalent to

$$Lu = \Phi_\xi(u). \tag{11}$$

⁷ Of course, in physical space, x and t , being angles, are defined modulus 2π , but to keep track of the topology (windings and rotations) one needs to consider them in the universal cover \mathbb{R} of $\mathbb{R}/(2\pi\mathbb{Z})$.

⁸ The procedure consists in reducing the problem to a fixed point problem containing parameters: The question is then solved by a Lyapunov–Schmidt or “range-bifurcation” decomposition. The “range equation” is solved by standard contraction mapping methods, but in order for the fixed point to correspond to a true solution of the original problem, a compatibility (zero-mean) condition has to be satisfied (“the bifurcation equation”), and this is done by exploiting a free parameter by means of a topological argument.

⁹ The parameter ξ is given by $(1/2\pi) \int_0^{2\pi} (x(qt) - pt) dt$ and will be our “bifurcation parameter.”

2.2 Step 2: The Green Operator $\mathcal{G} = L^{-1}$

Let C_{per}^k be the Banach space of 2π -periodic $C^k(\mathbb{R})$ functions endowed with the C^k -norm;¹⁰ let $C_{\text{per},0}^k$ be the closed subspace of C_{per}^k formed by functions with vanishing average over $[0, 2\pi]$; finally, denote by $\mathbb{B} := C_{\text{per},0}^0$ the Banach space of 2π -periodic continuous functions with zero average (endowed with the sup-norm).

The linear operator L defined in (10) maps injectively $C_{\text{per},0}^2$ onto \mathbb{B} ; the inverse operator (the ‘‘Green operator’’) $\mathcal{G} = L^{-1}$ is a bounded linear isomorphism. Indeed, the following elementary lemma holds:

Lemma 2.1 *Let $\hat{\eta} < 2/\pi$. Then¹¹*

$$\|\mathcal{G}\|_{L(\mathbb{B},\mathbb{B})} \leq \left(1 + \hat{\eta} \frac{\pi}{2} \left(1 - \hat{\eta} \frac{\pi}{2}\right)^{-1}\right) \frac{\pi^2}{8}.$$

In particular, assuming

$$\hat{\eta} \leq \frac{\pi}{5} \left(\frac{10}{\pi^2} - 1\right), \text{ i.e., } \eta \leq \begin{cases} \frac{\pi}{5} \left(\frac{10}{\pi^2} - 1\right) = 0.0083 \dots, & \text{if } (p, q) = (1, 1) \\ \frac{\pi}{10} \left(\frac{10}{\pi^2} - 1\right) = 0.0041 \dots, & \text{if } (p, q) = (3, 2) \end{cases} \tag{12}$$

one gets

$$\|\mathcal{G}\|_{L(\mathbb{B},\mathbb{B})} \leq \frac{5}{4}. \tag{13}$$

The proof of the above lemma is based on the following elementary result, whose proof is given in¹² Appendix 1:

Lemma 2.2

$$v \in C_{\text{per},0}^1 \implies \|v\|_{C^0} \leq \frac{\pi}{2} \|v'\|_{C^0} \tag{14}$$

$$v \in C_{\text{per},0}^2 \implies \|v\|_{C^0} \leq \frac{\pi^2}{8} \|v''\|_{C^0} \tag{15}$$

Proof of Lemma 2.1 Given $g \in \mathbb{B}$ with $\|g\|_{C^0} = 1$ we have to prove that, if $u \in C_{\text{per},0}^2$ is the unique solution of $u'' + \hat{\eta}u' = g$ with $\langle u \rangle = 0$, then

$$\|u\|_{C^0} \leq \left(1 + \hat{\eta} \frac{\pi}{2} \left(1 - \hat{\eta} \frac{\pi}{2}\right)^{-1}\right) \frac{\pi^2}{8}. \tag{16}$$

¹⁰ $\|v\|_{C^k} := \sup_{0 \leq j \leq k} \sup_{t \in \mathbb{R}} |D^j v(t)|$.

¹¹ $\|\mathcal{G}\|_{L(\mathbb{B},\mathbb{B})} = \sup_{u: \|u\|_{C^0}=1} \|\mathcal{G}(u)\|_{C^0}$.

¹² It is easy to see that the estimates in Lemma 2.2 are sharp.

We note that, setting $v := u'$, we have that $v \in \mathbb{B}$ and $v' = -\hat{\eta} v + g$. Then, we get

$$\|v\|_{C^0} \stackrel{(14)}{\leq} \frac{\pi}{2} \|-\hat{\eta} v + g\|_{C^0} \leq \frac{\pi}{2} (\hat{\eta} \|v\|_{C^0} + 1),$$

which implies

$$\|u'\|_{C^0} = \|v\|_{C^0} \leq \left(1 - \frac{\pi}{2} \hat{\eta}\right)^{-1} \frac{\pi}{2}. \tag{17}$$

Since $u'' = -\hat{\eta} u' + g$, we have

$$\|u\|_{C^0} \stackrel{(15)}{\leq} \frac{\pi^2}{8} \|-\hat{\eta} u' + g\|_{C^0} \leq \frac{\pi^2}{8} (1 + \hat{\eta} \|u'\|_{C^0}),$$

and (16) follows by (17). □

2.3 Step 3: Lyapunov–Schmidt Decomposition

Solutions of (11) are recognized as fixed points of the operator $\mathcal{G} \circ \Phi_\xi$:

$$u = \mathcal{G} \circ \Phi_\xi(u), \tag{18}$$

where ξ appears as a parameter.

To solve Eq. (18), we shall perform a *Lyapunov–Schmidt decomposition*. Let us denote by $\hat{\Phi}_\xi : C_{\text{per}}^0 \rightarrow \mathbb{B} = C_{\text{per},0}^0$ the operator

$$\begin{aligned} \hat{\Phi}_\xi(u) &:= \frac{1}{\hat{\varepsilon}} [\Phi_\xi(u) - \langle \Phi_\xi(u) \rangle] \\ &:= -f_x(\xi + pt + u(t), qt) + \phi_u(\xi), \end{aligned} \tag{19}$$

where

$$\phi_u(\xi) := \frac{1}{2\pi} \int_0^{2\pi} f_x(\xi + pt + u(t; \xi), qt) dt. \tag{20}$$

Then, Eq. (18) can be split into a “range equation”

$$u = \hat{\varepsilon} \mathcal{G} \circ \hat{\Phi}_\xi(u) \tag{21}$$

[where $u = u(\cdot; \xi)$] and a “bifurcation (or kernel) equation”

$$\phi_u(\xi) = \frac{\hat{\eta} \hat{v}}{\hat{\varepsilon}} \iff \langle \Phi_\xi(u(\cdot; \xi)) \rangle = 0. \tag{22}$$

Remark 2.3 (i) If $(u, \xi) \in \mathbb{B} \times [0, 2\pi]$ solves (21) and (22), then $x(t)$ solves (1).
 (ii) $\forall \xi \in [0, 2\pi], \hat{\Phi}_\xi \in C^1(\mathbb{B}, \mathbb{B})$; indeed, $\forall (u, \xi) \in \mathbb{B} \times [0, 2\pi]$,

$$\|\hat{\Phi}_\xi(u)\|_{C^0} \leq 2 \sup_{\mathbb{T}^2} |f_x|, \quad \|D_u \hat{\Phi}_\xi\|_{\mathcal{L}(\mathbb{B}, \mathbb{B})} \leq 2 \sup_{\mathbb{T}^2} |f_{xx}|. \tag{23}$$

The usual way to proceed to solve (21) and (22) is the following:

1. For any $\xi \in [0, 2\pi]$, find $u = u(\cdot; \xi)$ solving (21);
2. Insert $u = u(\cdot, \xi)$ into the kernel equation (22) and determine $\xi \in [0, 2\pi]$ so that (22) holds.

2.4 Step 4: Solving the Range Equation (Contracting Map Method)

For $\hat{\varepsilon}$ small the range equation is easily solved by standard contraction arguments.

Let $R := \frac{5}{2} \hat{\varepsilon} \sup_{\mathbb{T}^2} |f_x|$ and let

$$\begin{cases} \mathbb{B}_R := \{v \in \mathbb{B} : \|v\|_{C^0} \leq R\} \\ \varphi : v \in \mathbb{B}_R \rightarrow \varphi(v) := \hat{\varepsilon} \mathcal{G} \circ \hat{\Phi}_\xi(v). \end{cases} \tag{24}$$

Proposition 2.4 *Assume that $\hat{\eta}$ satisfies (12) and that*

$$\frac{5}{2} \hat{\varepsilon} \sup_{\mathbb{T}^2} |f_{xx}| < 1. \tag{25}$$

Then, for every $\xi \in [0, 2\pi]$, there exists a unique $u := u(\cdot; \xi) \in \mathbb{B}_R$ such that $\varphi(u) = u$.

Proof By (12) and (23) the map φ in (24) maps \mathbb{B}_R into itself and is a contraction with Lipschitz constant smaller than 1 by (25). The proof follows by the standard fixed point theorem. □

Recalling (3), (4), and (9), the “range condition” (25) writes

$$\varepsilon < \begin{cases} \frac{(1-\varepsilon)^3}{5}, & \text{if } (p, q) = (1, 1), \\ \frac{(1-\varepsilon)^3}{20}, & \text{if } (p, q) = (3, 2). \end{cases} \tag{26}$$

2.5 Step 5: Solving the Bifurcation Eq. (22)

The function $\phi_u(\xi)$ in (20) can be written as

$$\phi(\xi) = \phi^{(0)}(\xi) + \hat{\varepsilon} \tilde{\phi}_u^{(1)}(\xi; \hat{\varepsilon}) \tag{27}$$

with

$$\phi^{(0)}(\xi) := \frac{1}{2\pi} \int_0^{2\pi} f_x(\xi + pt, qt) dt. \tag{28}$$

By (24), for ε satisfying (26),

$$\sup_{\xi \in [0, 2\pi]} |\tilde{\phi}_u^{(1)}| \leq \sup_{\mathbb{T}^2} |f_{xx}| \frac{R}{\hat{\varepsilon}} \leq \frac{5}{2} \left(\sup_{\mathbb{T}^2} |f_x| \right) \left(\sup_{\mathbb{T}^2} |f_{xx}| \right). \tag{29}$$

By (3), (4), for ε satisfying (26), one finds immediately that

$$\sup_{\xi \in [0, 2\pi]} |\tilde{\phi}_u^{(1)}| \leq M_1 := \frac{5}{(1 - \mathbf{e})^6}. \tag{30}$$

Let us, now, have a closer look at the zero-order part $\phi^{(0)}$. The Newtonian potential f has the Fourier expansion

$$f(x, t) = \sum_{j \in \mathbb{Z}, j \neq 0} \alpha_j \cos(2x - jt), \tag{31}$$

where the Fourier coefficients $\alpha_j = \alpha_j(\mathbf{e})$ coincide with the Fourier coefficients of

$$G_{\mathbf{e}}(t) := -\frac{e^{2if_{\mathbf{e}}(t)}}{2\rho_{\mathbf{e}}(t)^3} = \sum_{j \in \mathbb{Z}, j \neq 0} \alpha_j \exp(ijt) \tag{32}$$

(see Appendix 2). Thus,

$$f_x(\xi + pt, qt) = -2 \sum_{j \in \mathbb{Z}, j \neq 0} \alpha_j \sin(2\xi + (2p - jq)t),$$

and one finds

$$\phi^{(0)}(\xi) = \begin{cases} -2\alpha_2 \sin(2\xi), & \text{if } (p, q) = (1, 1), \\ -2\alpha_3 \sin(2\xi), & \text{if } (p, q) = (3, 2). \end{cases} \tag{33}$$

Define

$$a_{pq} := \begin{cases} 2|\alpha_2| - \hat{\varepsilon}M_1, & \text{if } (p, q) = (1, 1), \\ 2|\alpha_3| - \hat{\varepsilon}M_1, & \text{if } (p, q) = (3, 2). \end{cases} \tag{34}$$

Then, from (27), (30), (33), and (34), it follows that $\phi([0, 2\pi])$ contains the interval $[-a_{pq}, a_{pq}]$, which is not empty provided [recall (9) and (30)]

$$\varepsilon < \begin{cases} \frac{2(1 - \mathbf{e})^6}{5} |\alpha_2(\mathbf{e})|, & \text{if } (p, q) = (1, 1), \\ \frac{(1 - \mathbf{e})^6}{10} |\alpha_3(\mathbf{e})|, & \text{if } (p, q) = (3, 2). \end{cases} \tag{35}$$

Therefore, we can conclude that the bifurcation equation (22) is solved if one assumes that $|\frac{\hat{\eta} \hat{\nu}}{\varepsilon}| \leq a_{pq}$, i.e. (recall again (9), (30), and (34)), if

$$\eta < \begin{cases} \frac{\varepsilon}{|v - 1|} \left(2|\alpha_2(\mathbf{e})| - \frac{5\varepsilon}{(1 - \mathbf{e})^6} \right), & \text{if } (p, q) = (1, 1), \\ \frac{2\varepsilon}{|2v - 3|} \left(2|\alpha_3(\mathbf{e})| - \frac{20\varepsilon}{(1 - \mathbf{e})^6} \right), & \text{if } (p, q) = (3, 2). \end{cases} \tag{36}$$

We have proven the following:

Proposition 1 *Let $(p, q) = (1, 1)$ or $(p, q) = (3, 2)$ and assume (12), (26), (35), and (36). Then, (1) admits $p:q$ spin-orbit resonances $x(t)$ as in (7).*

2.6 Step 6: Lower Bounds on $|\alpha_2(\mathbf{e})|$ and $|\alpha_3(\mathbf{e})|$

In order to complete the proof of the theorem, by checking the conditions of Proposition 1 for the resonant satellites of the Solar System, we need to give lower bounds on the absolute values of the Fourier coefficients $\alpha_2(\mathbf{e})$ and $\alpha_3(\mathbf{e})$. To do this we will simply use a Taylor formula to develop $\alpha_j(\mathbf{e})$ in powers of \mathbf{e} up to suitably large order¹³

$$\alpha_j(\mathbf{e}) = \sum_{k=0}^h \alpha_j^{(k)} \mathbf{e}^k + R_j^{(h)}(\mathbf{e}) \tag{37}$$

and use the analyticity property of $G_{\mathbf{e}}$ to get an upper bound on $R_j^{(h)}$ by means of standard Cauchy estimates for holomorphic functions. To use Cauchy estimates, we need an upper bound of $G_{\mathbf{e}}$ in a complex eccentricity region. The following simple result will be enough:

Lemma 2 *Fix $0 < b < 1$. The solution $u_{\mathbf{e}}(t)$ of the Kepler equation (5) is, for every $t \in \mathbb{R}$, holomorphic with respect to \mathbf{e} in the complex disk*

$$|\mathbf{e}| < e_* := \frac{b}{\cosh b} \tag{38}$$

and satisfies

$$\sup_{t \in \mathbb{R}} |u_{\mathbf{e}}(t) - t| \leq b. \tag{39}$$

¹³ We shall choose $h = 4$ for the 1:1 resonances and $h = 21$ for the 3:2 case of Mercury.

Moreover, $\rho_{\mathbf{e}}(t) = 1 - \mathbf{e} \cos(u_{\mathbf{e}}(t))$ satisfies

$$|\rho_{\mathbf{e}}(t)| \geq 1 - b, \quad \forall t \in \mathbb{R}, \quad |\mathbf{e}| < e_* \tag{40}$$

and $G_{\mathbf{e}}(t)$ (defined in (32)) satisfies

$$|G_{\mathbf{e}}(t)| \leq \frac{2}{(1-b)^5} (|1 - \mathbf{e}|(1 + \cosh b) + 1 - b)^2, \quad \forall t \in \mathbb{R}, \quad |\mathbf{e}| < e_* \tag{41}$$

Proof Using that

$$\sup_{|\operatorname{Im} z| < b} |\sin z| = \sup_{|\operatorname{Im} z| < b} |\cos z| = \cosh b, \tag{42}$$

one sees that for $|\mathbf{e}| < e_*$ the map $v \mapsto \chi_{\mathbf{e}}(v)$ with $[\chi_{\mathbf{e}}(v)](t) := \mathbf{e} \sin(v(t) + t)$ is a contraction in the closed ball of radius b in the space of continuous functions endowed with the sup-norm. Moreover, since $\chi_{\mathbf{e}}(v)$ is holomorphic in \mathbf{e} , the same holds for the fixed point $v_{\mathbf{e}}(t)$ of $\chi_{\mathbf{e}}$. The estimate in (39) follows by observing that $u_{\mathbf{e}}(t) = v_{\mathbf{e}}(t) + t$. Since by (39) we get

$$|\operatorname{Im}(u_{\mathbf{e}}(t))| \leq b, \quad \forall t \in \mathbb{R}, \quad |\mathbf{e}| < e_*, \tag{43}$$

estimate (40) follows by

$$|\rho_{\mathbf{e}}(t)| \geq 1 - |\mathbf{e}| |\cos(u_{\mathbf{e}}(t))| \stackrel{(42)}{\geq} 1 - e_* \cosh b = 1 - b.$$

Next, let $w_{\mathbf{e}}(t) := \sqrt{\frac{1+\mathbf{e}}{1-\mathbf{e}}} \tan\left(\frac{u_{\mathbf{e}}(t)}{2}\right)$ so that $f_{\mathbf{e}} = 2 \arctan w_{\mathbf{e}}$. Then,¹⁴

$$|e^{2if_{\mathbf{e}}(t)}| = \frac{|w - i|^4}{|w^2 + 1|^2} \leq \left(\frac{4}{|w^2 + 1|} + 2\right)^2 = 4 \left(\frac{|1 - \mathbf{e}| |1 + \cos u_{\mathbf{e}}|}{|1 - \mathbf{e} \cos u_{\mathbf{e}}|} + 1\right)^2.$$

Then, (41) follows by (40), (42), and (43).

Lemma 3 Let $R_j^{(h)}(\mathbf{e})$ be as in (37), $0 < b < 1$, and $0 < \mathbf{e} < b / \cosh b$. Then,

$$|R_j^{(h)}(\mathbf{e})| \leq R^{(h)}(\mathbf{e}; b)$$

with

$$R^{(h)}(\mathbf{e}; b) := \frac{2}{(1-b)^5} \times \left(\left(1 + \frac{b}{\cosh b} - \mathbf{e} \right) (1 + \cosh b) + 1 - b \right)^2 \frac{\mathbf{e}^{h+1}}{\left(\frac{b}{\cosh b} - \mathbf{e} \right)^{h+1}}.$$

¹⁴ Use $e^{2iz} = \frac{i-w}{w+i} = -\frac{(w-i)^2}{w^2+1}$ and $\tan^2(\alpha/2) = (1 - \cos \alpha)/(1 + \cos \alpha)$.

Proof For $\mathbf{e}, \rho > 0$ we set

$$[0, \mathbf{e}]_\rho := \{ z \in \mathbb{C}, \text{ s.t. } z = z_1 + z_2, z_1 \in [0, \mathbf{e}], |z_2| < \rho \}.$$

Lemma 2 and standard (complex) Cauchy estimates imply, for $0 \leq s \leq 1$,

$$|D^{h+1} \alpha_j(s\mathbf{e})| \leq \frac{(h+1)!}{(e_* - \mathbf{e})^{h+1}} \sup_{[0, \mathbf{e}]_{e_* - \mathbf{e}}} |\alpha_j|$$

and, therefore,

$$|R_j^{(h)}(\mathbf{e})| \leq \frac{\mathbf{e}^{h+1}}{(e_* - \mathbf{e})^{h+1}} \sup_{[0, \mathbf{e}]_{e_* - \mathbf{e}}} |\alpha_j|.$$

By (41) we obtain

$$\sup_{[0, \mathbf{e}]_{e_* - \mathbf{e}}} |\alpha_j| \leq \frac{2}{(1-b)^5} ((1 + e_* - \mathbf{e})(1 + \cosh b) + 1 - b)^2$$

from which, recalling (38), the lemma follows.

Now, in order to check the conditions of Proposition 1, we will expand α_2 in powers of \mathbf{e} up to order $h = 4$ and α_3 up to order $h = 21$. Using the representation formula (53) for the α_j given in Appendix 2, we find

$$\begin{aligned} \alpha_2(\mathbf{e}) &= -\frac{1}{2} + \frac{5}{4}\mathbf{e}^2 - \frac{13}{32}\mathbf{e}^4 + R_2^{(4)}(\mathbf{e}), \\ \alpha_3(\mathbf{e}) &= -\frac{7}{4}\mathbf{e} + \frac{123}{32}\mathbf{e}^3 - \frac{489}{256}\mathbf{e}^5 + \frac{1763}{4096}\mathbf{e}^7 - \frac{13527}{327680}\mathbf{e}^9 + \frac{180369}{13107200}\mathbf{e}^{11} \\ &\quad + \frac{5986093}{734003200}\mathbf{e}^{13} + \frac{24606987}{3355443200}\mathbf{e}^{15} + \frac{33790034193}{5261334937600}\mathbf{e}^{17} \\ &\quad + \frac{1193558821627}{210453397504000}\mathbf{e}^{19} + \frac{467145991400853}{92599494901760000}\mathbf{e}^{21} + R_3^{(21)}(\mathbf{e}). \end{aligned}$$

In view of Lemma 3, we choose, respectively, $b = 0.462678$ and¹⁵ $b = 0.768368$ to get lower bounds:

$$|\alpha_2(\mathbf{e})| \geq \left| \frac{1}{2} - \frac{5}{4}\mathbf{e}^2 + \frac{13}{32}\mathbf{e}^4 \right| - |R^{(4)}(\mathbf{e}; 0.462678)| \tag{44}$$

$$|\alpha_3(\mathbf{e})| \geq \left| \sum_{k=1}^{21} \alpha_3^{(k)} \mathbf{e}^k \right| - |R^{(21)}(\mathbf{e}; 0.768368)|. \tag{45}$$

¹⁵ The values for b are rather arbitrary (as long as $0 < b < 1$); our choice is made for optimizing the estimates.

Table 3 Check of the hypotheses of Proposition 1 for the satellites in spin–orbit resonance

Satellite	Lower bound on $ \alpha_q $	r.h.s.–l.h.s. of Eq. (26)	r.h.s.–l.h.s. of Eq. (35)	r.h.s. of Eq. (36)
Moon	0.45475265	0.1663508	0.127144	0.1225335
Io	0.49997893	0.1889174	0.186489	81.800325
Europa	0.49988598	0.1934518	0.187978	1.8031043
Ganymede	0.49999849	0.1974024	0.196745	264.3751
Callisto	0.49993049	0.1937258	0.189389	5.6260606
Mimas	0.49938883	0.0989819	0.088051	19.852395
Enceladus	0.49997228	0.161793	0.159015	218.44519
Tethys	0.49999999	0.1670079	0.166948	458437.46
Dione	0.49999395	0.1901481	0.188837	281.18521
Rhea	0.49999875	0.1895878	0.18899	1554.7362
Titan	0.49776167	0.1830341	0.166905	0.0357326
Iapetus	0.49790449	0.171834	0.155986	2.2484865
Ariel	0.4999982	0.1871186	0.186401	1321.448
Umbriel	0.499998095	0.1833031	0.180992	145.83674
Titania	0.49999849	0.1924958	0.191838	910.34423
Oberon	0.49999755	0.188917	0.188081	826.10305
Miranda	0.49999789	0.1505305	0.149754	3623.6286
Charon	0.49999395	0.1917247	0.190414	231.15781
Mercury	0.27	0.0244515	0.006171	0.0012363

2.7 Step 7: Check of the Conditions and Conclusion of the Proof

We are now ready to check all conditions of Proposition 1 with the parameters of the satellites in spin–orbit resonance given in Tables 1 and 2.

In Table 3 we report:

In column 2: the lower bounds on $|\alpha_q(\mathbf{e})|$ as obtained in step 6 using (44) and (45) (with the eccentricities listed in Tables 1 and 2)

In column 3: the difference between the right-hand side and the left-hand side of the inequality¹⁶ (26)

In column 4: the difference between the right-hand side and the left-hand side of the inequality (35)

In column 5: the right-hand side of the inequality (36), which is an upper bound for the admissible values of the dissipative parameter η

The positive values reported in the third and fourth column mean that the range condition (26) and the topological condition (35) are satisfied for all the moons in 1:1 resonance and for Mercury; the bifurcation condition (36) yields an upper bound on the admissible value for η (fifth column). Thus, η has to be smaller than the minimum

¹⁶ Thus, the inequality is satisfied if the numerical value in the column is positive; the same applies to the fifth column.

between the value in the fifth column of Table 3 and the value in the right-hand side of Eq. (12) (needed to give a bound on the Green operator): this minimum value is 0.008 for the moons in 1:1 resonance and 0.001 for Mercury.

The proof of the theorem is complete.

Acknowledgments We thank J. Castillo-Rogez, A. Celletti, M. Efroimsky, and F. Nimmo for useful discussions. Partially supported by the MIUR grant “Critical Point Theory and Perturbative Methods for Nonlinear Differential Equations” (PRIN2009).

Appendix 1: Proof of Lemma 2.2

Proof We first prove (14). Up to a rescaling we can prove (14) assuming $\|v'\|_{C^0} = 1$. Assume by contradiction that

$$\|v\|_{C^0} =: c > \pi/2.$$

Note that it is obvious that $c \leq \pi$, since v has zero average and, therefore, must vanish at some point. Since $|v|$ is a continuous periodic function it attains a maximum at some point; up to a translation we can assume that $|v|$ attains its maximum in $-c$. In that case, multiplying by -1 , we can also assume that $-c$ is a minimum, namely

$$\|v\|_{C^0} = c = -v(-c).$$

Since $\|v'\|_{C^0} = 1$, we get

$$v(t) \leq -c + |t + c|, \quad \forall t \in [-2c, 0]$$

and, therefore,

$$v(0) \leq 0, \quad v(-2c) \leq 0, \quad \int_{-2c}^0 v \leq -c^2. \tag{46}$$

Since $\|v'\|_{C^0} = 1$, we also get

$$v(t) \leq \pi - c - |t - \pi + c|, \quad \forall t \in [0, 2\pi - 2c].$$

Then,

$$\int_0^{2\pi-2c} v \leq (\pi - c)^2.$$

Combining with the last inequality in (46), we get

$$\int_{-2c}^{2\pi-2c} v \leq (\pi - c)^2 - c^2 = \pi(\pi - 2c) < 0,$$

which contradicts the fact that v has zero average, proving (14).

We now prove (15). Up to a rescaling we can prove (15) assuming $\|v''\|_{C^0} = 1$. Assume by contradiction that

$$\|v\|_{C^0} =: c > \pi^2/8. \tag{47}$$

Up to a translation we can assume that $|v|$ attains maximum at 0. In that case, multiplying by -1 , we can also assume that $-c$ is a minimum, namely

$$\|v\|_{C^0} = c = -v(0).$$

Since $\|v''\|_{C^0} = 1$, we get

$$v(t) \leq -c + t^2/2, \quad \forall t \in \mathbb{R}.$$

Since v has zero average must exist $t_1 < 0 < t_2$

$$s.t. v(t_1) = v(t_2) = 0, v(t) < 0 \forall t \in (t_1, t_2), \tag{48}$$

Moreover,

$$\text{and } t_1 \leq -\sqrt{2c}, t_2 \geq \sqrt{2c}, t_2 - t_1 < 2\pi.$$

Since v has zero average and is 2π -periodic,

$$\int_{t_2}^{2\pi+t_1} v = - \int_{t_1}^{t_2} v \geq \frac{2}{3}(2c)^{3/2}. \tag{49}$$

Set

$$a := \pi + (t_1 - t_2)/2$$

and note that

$$0 < a \leq \pi - \sqrt{2c} < \pi/2, \quad a^2 < 2c \tag{50}$$

by (48) and (47). Set

$$u(t) := v(t + \pi + (t_1 + t_2)/2).$$

Note that $u \in \mathbb{B} \cap C^2$ and, by (48),

$$\|u\|_{C^0} = c, \quad \|u''\|_{C^0} = 1, \quad u(-a) = u(a) = 0, \quad \int_{-a}^a u = \int_{t_2}^{2\pi+t_1} v \stackrel{(49)}{\geq} \frac{2}{3}(2c)^{3/2}.$$

Consider now the even function

$$w(t) := \frac{1}{2}(u(t) + u(-t)).$$

Note that $w \in \mathbb{B} \cap C^2$ and

$$\|w\|_{C^0} \leq c, \quad \|w''\|_{C^0} \leq 1, \quad w(-a) = 0, \quad \int_{-a}^0 w = \frac{1}{2} \int_{-a}^a u \geq \frac{1}{3}(2c)^{3/2}. \quad (51)$$

Set

$$z(t) := c - \frac{c}{a^2}t^2.$$

We claim that

$$z(t) \geq w(t), \quad \forall -a \leq t \leq 0. \quad (52)$$

Then,

$$\int_{-a}^0 w \leq \int_{-a}^0 z = \frac{2}{3}ca \stackrel{(50)}{<} \frac{1}{3}(2c)^{3/2} \stackrel{(51)}{\leq} \int_{-a}^0 w,$$

which is a contradiction.

Let us prove the claim in (52). Note that $z(-a) = w(-a) = 0$. Assume by contradiction that there exists $\bar{t} \in [-a, 0)$ such that

$$z(\bar{t}) = w(\bar{t}), \quad z(t) \geq w(t), \quad \forall t \in [-a, \bar{t}], \quad z'(\bar{t}) \leq w'(\bar{t}).$$

Then, since $\|w''\|_{C^0} \leq 1$,

$$\begin{aligned} w(t) &\geq w(\bar{t}) + w'(\bar{t})(t - \bar{t}) - \frac{1}{2}(t - \bar{t})^2 \\ &\stackrel{(50)}{>} z(\bar{t}) + z'(\bar{t})(t - \bar{t}) - \frac{c}{a^2}(t - \bar{t})^2 = z(t), \quad \forall t \in (\bar{t}, 0]. \end{aligned}$$

Then,

$$w(0) > z(0) = c,$$

which contradicts the first inequality in (51). This completes the proof of (15). \square

Appendix 2: Fourier Coefficients of the Newtonian Potential

Properties of the Fourier coefficients α_j of the Newtonian potential f , including Eq. (32), have been discussed, e.g., in Appendix 1 of¹⁷ [Biasco and Chierchia \(2009\)](#).

Here we provide a simple formula for the Fourier coefficients α_j of the Newtonian potential f in (3) [compare (d) of §1, and (31)–(32)]; namely we prove that

$$\alpha_j = -\frac{1}{4\pi} \int_0^{2\pi} \frac{1}{\rho^2(w^2 + 1)^2} \left[(w^4 - 6w^2 + 1)c_j(u) - 4w(w^2 - 1)s_j(u) \right] du, \tag{53}$$

where $w = w(u; \mathbf{e}) := \sqrt{\frac{1+\mathbf{e}}{1-\mathbf{e}}} \tan \frac{u}{2}$, $\rho = 1 - \mathbf{e} \cos u$, and

$$c_j(u) := \cos(ju - j\mathbf{e} \sin u), \quad s_j(u) := \sin(ju - j\mathbf{e} \sin u).$$

Proof If $z = \arctan w$, then

$$e^{2iz} = \frac{i - w}{w + i} = -\frac{(w - i)^2}{w^2 + 1}, \tag{54}$$

so that if $w_{\mathbf{e}}(t) := w(u_{\mathbf{e}}(t), \mathbf{e})$ one has $f_{\mathbf{e}} = 2 \arctan w_{\mathbf{e}}$ and

$$\begin{aligned} G_{\mathbf{e}} &= -\frac{1}{2\rho_{\mathbf{e}}^3} \frac{(w_{\mathbf{e}} - i)^2}{(w_{\mathbf{e}} + i)^2} = -\frac{1}{2\rho_{\mathbf{e}}^3} \frac{(w_{\mathbf{e}} - i)^4}{(w_{\mathbf{e}}^2 + 1)^2} \\ &= -\frac{1}{2\rho_{\mathbf{e}}^3} \frac{1}{(w_{\mathbf{e}}^2 + 1)^2} \left(w_{\mathbf{e}}^4 - 6w_{\mathbf{e}}^2 + 1 - 4i w_{\mathbf{e}}(w_{\mathbf{e}}^2 - 1) \right). \end{aligned} \tag{55}$$

By parity properties, it is easy to see that the G_j 's are real, namely $G_j = \bar{G}_j$, so that

$$\begin{aligned} \alpha_j = G_j &= \frac{1}{2\pi} \int_0^{2\pi} G(t) e^{-ijt} dt = -\frac{1}{4\pi} \int_0^{2\pi} \frac{e^{i2f_{\mathbf{e}}(t)-ijt}}{\rho_{\mathbf{e}}(t)^3} dt \\ &= -\frac{1}{4\pi} \int_0^{2\pi} \frac{1}{\rho_{\mathbf{e}}^3(w_{\mathbf{e}}^2 + 1)^2} \left[(w_{\mathbf{e}}^4 - 6w_{\mathbf{e}}^2 + 1) \cos(jt) - 4w_{\mathbf{e}}(w_{\mathbf{e}}^2 - 1) \sin(jt) \right] dt. \end{aligned}$$

¹⁷ A factor $-1/2$ is missing in the definition of $G(t)$ given in [Biasco and Chierchia \(2009\)](#), (iii) p. 4366 and, consequently, it has to be included at p. 4367 in line 6 (from above, counting also lines with formulas) in front of “Re”; in line 12, 17, and 18 the factor $1/(2\pi)$ has to be replaced by $-1/(4\pi)$.

Making the change of variable given by the Kepler equation (5), i.e., integrating from t to $u = u_e$ and setting $u_e(t)' = \frac{1}{\rho_e(t)}$, one gets (53). \square

Appendix 3: Small Bodies

In the Solar System, besides the 18 moons listed in Table 1 and Mercury, there are five other minor bodies with mean radius smaller than 100 km observed in 1:1 spin-orbit resonance around their planet: Phobos and Deimos (Mars), Amalthea (Jupiter), and Janus and Epimetheus (Saturn), as listed in Table 4.

Besides being small, such bodies have also a quite irregular shape and only Janus and Epimetheus have good equatorial symmetry.¹⁸ Indeed, for these two small moons (and only for them among the minor bodies), our theorem holds as shown by the data reported in Table 5.¹⁹

Table 4 Physical data of minor bodies in 1:1 spin-orbit resonance

Principal body	Satellite	Eccentricity e	a (km)	b (km)	Oblateness $\varepsilon = \frac{3}{2} \frac{a^2 - b^2}{a^2 + b^2}$	ν
Mars	Phobos ^{a,b}	0.0151	13.4	11.2	0.26616393443	1.00136808
	Deimos ^{a,b}	0.0002	7.5	6.1	0.30558527712	1.00000024
Jupiter	Amalthea ^a	0.0031	125	73	0.73704304667	1.00005766
Saturn	Janus ^c	0.0073	97.4	96.9	0.00771996946	1.000319741
	Epimetheus ^c	0.0205	58.7	58.0	0.01799421119	1.002521568

^a Thomas et al. (1998)

^b Thomas (1989) and <http://solarsystem.nasa.gov/planets/profile.cfm?Object=Mars&Display=Sats>

^c Porco et al. (2007)

Table 5 Check of the hypotheses of Proposition 1 for the small satellites in spin-orbit resonance

Satellite	Lower bound on $ \alpha_q $	r.h.s.–l.h.s. of Eq. (26)	r.h.s.–l.h.s. of Eq. (35)	r.h.s. of Eq. (36)
Janus	0.4999324	0.1879319	0.183652	23.167321
Epimetheus	0.49927518	0.1699562	0.158377	6.3987689

¹⁸ For pictures, see: <http://photojournal.jpl.nasa.gov/catalog/PIA10369> (Phobos), <http://photojournal.jpl.nasa.gov/catalog/PIA11826> (Deimos), <http://photojournal.jpl.nasa.gov/catalog/PIA02532> (Amalthea), <http://photojournal.jpl.nasa.gov/catalog/PIA12714> (Janus), <http://photojournal.jpl.nasa.gov/catalog/PIA12700> (Epimetheus).

¹⁹ Positive values in the third and fourth column and values less than 0.008 in the fifth column imply that the assumptions of Proposition 1 hold.

References

- Bambusi, D., Haus, E.: Asymptotic stability of synchronous orbits for a gravitating viscoelastic sphere. *Celest. Mech. Dyn. Astron.* **114**(3), 255–277 (2012)
- Biasco, L., Chierchia, L.: Low-order resonances in weakly dissipative spin–orbit models. *J. Differ. Equ.* **246**, 4345–4370 (2009)
- Castillo-Rogez, J.C., Efroimsky, M., Lainey, V.: The tidal history of Iapetus: spin dynamics in the light of a refined dissipation mode. *J. Geophys. Res.* **116**, E09008 (2011). doi:[10.1029/2010JE003664](https://doi.org/10.1029/2010JE003664)
- Celletti, A.: Analysis of resonances in the spin–orbit problem in celestial mechanics: the synchronous resonance (part I). *J. Appl. Math. Phys.* **41**, 174–204 (1990)
- Celletti, A.: *Stability and Chaos in Celestial Mechanics*. Springer-Praxis, Providence (2010)
- Celletti, A., Chierchia, L.: Quasi-periodic attractors in celestial mechanics. *Arch. Ration. Mech. Anal.* **191**(2), 311–345 (2009)
- Correia, A.C.M., Laskar, J.: Mercury’s capture into the 3/2 spin–orbit resonance as a result of its chaotic dynamics. *Nature* **429**, 848–850 (2004)
- Danby, J.M.A.: *Fundamentals of Celestial Mechanics*. Macmillan, New York (1962)
- Dougherty, M.K., et al. (eds.): *Saturn from Cassini–Huygens*. Springer, Netherlands (2009). doi:[10.1007/978-1-4020-9217-6](https://doi.org/10.1007/978-1-4020-9217-6)
- Goldreich, P., Peale, S.: Spin–orbit coupling in the solar system. *Astron. J.* **71**, 425 (1967)
- Husmann, H., Sohl, F., Spohn, T.: Subsurface oceans and deep interiors of medium-sized outer planet satellites and large trans-neptunian objects. *Icarus* **185**, 258–273 (2006)
- Iess, L., et al.: Gravity field, shape, and moment of inertia of Titan. *Science* **327**, 1367–1369 (2010)
- Iess, L., et al.: The tides of Titan. *Science* **337**(6093), 457–459 (2012)
- Lainey, V., et al.: Strong tidal dissipation in Saturn and constraints on Enceladus’ thermal state from astrometry. *Astrophys. J.* **752**(1), 14–19 (2012)
- MacDonald, G.J.F.: Tidal friction. *Rev. Geophys.* **2**, 467–541 (1964)
- Peale, S.J.: The free precession and libration of Mercury. *Icarus* **178**, 4–18 (2005)
- Porco, C.C., et al.: Saturn’s small inner satellites: clues to their origins. *Science* **318**, 1602–1607 (2007)
- Runcorn, S.K., Hofmann, S.: The Moon. In: *Proceedings from IAU Symposium no. 47*. Reidel, Dordrecht (1972)
- Sicardy, B., et al.: Charon’s size and an upper limit on its atmosphere from a stellar occultation. *Nature* **439**, 52–54 (2006)
- Thomas, P.C.: Radii, shapes, and topography of the satellites of Uranus from limb coordinates. *Icarus* **73**, 427–441 (1988)
- Thomas, P.C.: The shapes of small satellites. *Icarus* **77**, 248–274 (1989)
- Thomas, P.C., et al.: The small inner satellites of Jupiter. *Icarus* **135**, 360–371 (1998)
- Wintner, A.: *The Analytic Foundations of Celestial Mechanics*. Princeton University Press, Princeton (1941)
- Wisdom, J.: Rotational dynamics of irregularly shaped natural satellites. *Astron. J.* **94**(5), 1350–1360 (1987)